

# A long-term climatology of North Atlantic polar lows

Matthias Zahn<sup>1,2</sup> and Hans von Storch<sup>1,2</sup>

Received 21 August 2008; revised 24 September 2008; accepted 10 October 2008; published 20 November 2008.

[1] A dynamical downscaling of the 6-hourly 1948–2006 NCEP/NCAR re-analyses for the subarctic region of the North Atlantic has been used to derive a climatology of polar lows by means of a tracking algorithm based on the simulated bandpass filtered MSLP-fields. This climatology is consistent with the limited observational evidence in terms of frequency and spatial distribution. The climatology exhibits strong year-to-year variability but weak decadal variability and a negligible trend. A Canonical Correlation Analysis describes the conditioning of the formation of polar lows by characteristic meridional seasonal mean flow regimes, which favor cold air outbreaks and upper air troughs. **Citation:** Zahn, M., and H. von Storch (2008), A long-term climatology of North Atlantic polar lows, *Geophys. Res. Lett.*, 35, L22702, doi:10.1029/2008GL035769.

## 1. Introduction

[2] Polar lows [Rasmussen and Turner, 2003] are severe maritime mesoscale storms in sub polar regions with wind speed around and above gale force.

[3] Since the availability of comprehensive observations supported by satellite imagery, a couple of authors dealt with climatological issues of polar lows [Businger, 1985; Wilhelmsen, 1985; Noer and Ovsted, 2003; Blechschmidt, 2008]. However these observation based studies lack a sufficiently long enough time series of polar low occurrences and might also suffer from inhomogeneities due to the subjective way of data recording for robust statements on trends and variability of polar lows.

[4] So far the requirement of a sufficiently long and homogeneous time series is only fulfilled by numerical reanalysis data. Thus a number of further authors have applied global reanalysis data to investigate characteristics of polar lows statistics recently. Condron *et al.* [2006] located the Laplacian of the pressure field or geopotential height in relatively coarsely gridded reanalysis data to detect mesocyclones and investigate their frequency. To overcome the problem of too coarsely resolved data in the global reanalysis products Kolstad [2006] identifies low static stability and reverse wind shear conditions in the ERA40 reanalyses [Simmons and Gibson, 2000] indicative for reverse shear polar lows. Similarly Claud *et al.* [2007] made use of different indicators for polar lows in reanalysis fields (NCEP and ERA40), which they related to various low frequency patterns of the atmosphere. By applying a cold air outbreak indicator and a vorticity constraint to

numerical weather prediction data, Bracegirdle and Gray [2008] managed to identify individual polar low events in the North Atlantic. However, their data spanned a short time (2000–2004) and it was not possible to track polar lows in the 12 hourly output fields. A cold air outbreak indicator was also used as an indirect measure of polar low activity by Kolstad *et al.* [2008].

[5] In this paper we make use of the coarsely resolved large scale atmospheric fields of the NCEP/NCAR global reanalyses [Kalnay *et al.*, 1996], but we downscale them with a higher resolution local area model (LAM) for a period of almost 60 years. That individual polar low cases are by and large reproducible with such an approach has been shown [Zahn *et al.*, 2008]. However, the core pressures are too high compared to synoptic analyses but considerably deeper than in the driving re-analyses. The same is true for wind speeds.

[6] Zahn and von Storch [2008] (hereinafter referred to as ZvS08) exploited two dimensional digital bandpass filters [Feser and von Storch, 2005] to develop an automated detection procedure to track polar lows over a two year period and showed that statistics of polar lows in terms of frequency and spatial distribution can be derived with such an approach. Here we use the same algorithm to extend this work to a longer time period, from 1948 through 2006. This enables the compilation of a long term data base of polar lows for the first time. In this paper we use this data base to investigate trends and variability of polar low occurrences in the North Atlantic and their linkage to the large scale pressure situation over the last 60 years.

## 2. Data and Methodology

[7] The LAM we applied in this study is the CLM, the climate version of the “Lokal Modell” of the German Weather service [Böhm *et al.*, 2006]. As initial and lateral boundary values, we used the NCEP/NCAR re-analyses [Kalnay *et al.*, 1996]. The NCEP-large scale situation is enforced through spectral nudging [von Storch *et al.*, 2000] to prevent CLM significantly deviating from the analyzed large scale state. Sea surface temperature and sea ice extent were also prescribed according to the NCEP/NCAR re-analyses. The simulation period starts 1 January 1948 and lasts through February 2006. The simulation area covers the whole North Atlantic including the Labrador Sea west of Greenland and the Barents Sea in the East, the ice edge prone to shallow baroclinicity in the North and about the position of the Polar Front in the South (cf. Figure 1 of ZvS08).

[8] The objective detection procedure of ZvS08 was applied to the simulated output fields. The detection procedure searches for the minima in the bandpass filtered mean sea level pressure (MSLP) fields and concatenates the minima in consecutive time steps to tracks. Along these

<sup>1</sup>Institute for Coastal Research, GKSS Research Center, Geesthacht, Germany.

<sup>2</sup>Meteorological Institute, University of Hamburg, Hamburg, Germany.

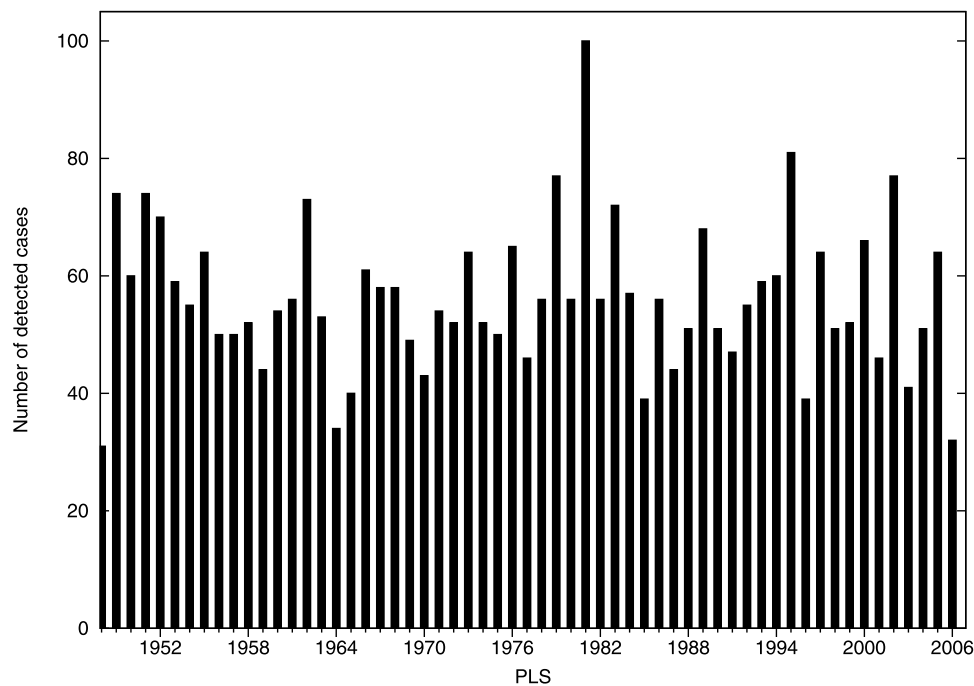


**Figure 1.** Number of detected polar lows per polar low season. One polar low season is defined as the period starting 1 July and ending 30 June the following year.

tracks, the fulfillment of further criteria are requested: (1) strength of the minimum ( $\leq -2$  hPa once along the track), (2) wind speed ( $\geq 13.9 \frac{m}{s}$  once along the track), (3) air-sea temperature difference ( $\delta SST - T_{500 \text{ hPa}} \geq 43 \text{ K}$ ), (4) north south direction of the track, and (5) limits to allowable adjacent grid boxes.

[9] When the strength of the minimum in the bandpass filtered MSLP field decreases below  $-6 \text{ hPa}$  once, and there are not too many coastal grid boxes around that location, a polar low is recorded independent of the other criteria.

### 3. Results

[10] Polar lows are winter phenomena which in general occur in the period from October through May. Therefore, we use the term “Polar Low Season” (PLS) to describe the one year period from July through June the following year. A polar low season is addressed by the second year, e.g. the PLS 1950 begins in July 1949 and ends June 1950. PLSs 1948 and 2006 are omitted from our statistical analysis, as they do not contain the whole number of 12 months.

#### 3.1. Trends and Variability

[11] Figure 1 shows the yearly time series of the number of detected polar lows per PLS. 3313 polar lows resulted in a mean number of approx. 56 polar lows for each PLS with a strong year-to-year variability indicated by a standard deviation of  $\sigma \approx \pm 13$ . Maximum and minimum numbers of detected cases are found in PLS 1981 with 100 cases and 1964 with only 34 cases.

[12] The decadal variability is weak. The overall trend in the frequency of polar lows is negligible with  $-0.024$  cases/year. Also, the slope of the trend strongly depends on the number of cases of the first/last PLSs.

[13] The annual cycle of monthly numbers of detected polar lows reveals highest frequency in winter with maxima in December and January and almost no polar low activity in summer (not shown). Contrary to other authors [e.g., *Wilhelmsen*, 1985; *Lystad*, 1986; *ZvS08*; *Noer and Ovhed*, 2003] no secondary minimum of polar low activity in February compared to January and March is found in our investigations for the whole period. However *Wilhelmsen* [1985] and *Lystad* [1986] only focused on the northern North Atlantic close to Norway during a few winters. When we extract activity in equivalent periods and regions these secondary minima become visible in our data too, (not shown). Similarly a secondary minimum is evident for polar low activity in PLSs 1993 through 1995 (cf. *ZvS08*), but not for period and region used by *Noer and Ovhed* [2003].

[14] The spatial distribution of polar low occurrences is plotted in Figure 2. The location of each polar low is defined as the location at which its track is detected for the first time. Highest absolute frequency and frequency per maritime area are found in the region south and east of Iceland in accordance with investigations of *Harold et al.* [1999] or *Condron et al.* [2006]. Although *Bracegirdle and Gray* [2008] mainly focus their investigations on the North Atlantic around Norway, they also detect a maximum of possible polar lows in the Iceland-Greenland region.

[15] A second maximum in counts per maritime area unit is found in the northern North Atlantic regions, R7 and R2, which is also in accordance with the above mentioned studies and with *Kolstad* [2006].

[16] Also for the different regions, only negligible trends and high year-to-year variability for polar low frequency are found. Almost all regions (apart from R5 and R8) have PLSs without polar low activity but also PLSs with high activity (not shown).

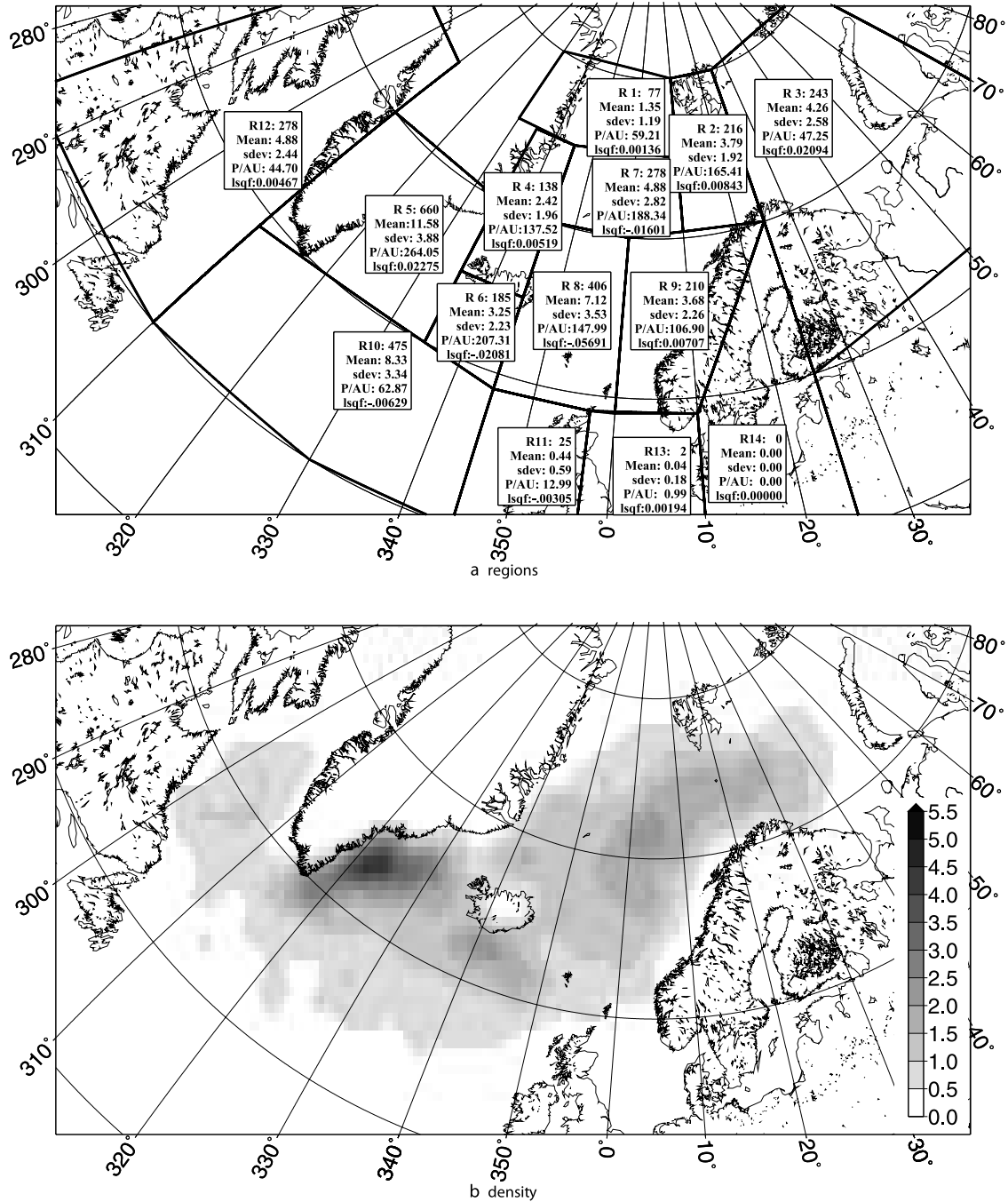


**Figure 2.** (a) Subregions, for which the number of detected polar lows were counted (R1–R14) and respective number of detected polar lows (see text). Difference in total number of polar lows (3313) and sum of polar lows in the respective regions (3193) is due to polar lows occurring in the Southwest outside the investigated area. Also given for each region are mean number of polar lows per year (Mean), standard deviation (sdev), slope of least squares fit (lsqf) and polar lows per area unit (P/AU). The latter number is normalised by the smallest region in terms of surface area, R6, and divided by the respective region's fraction of maritime boxes in the model. (b) Polar low density distribution. Unit: detected polar lows per  $250 \text{ km}^2$ .

[17] We further examined the sensitivity of the time series regarding the thresholds prescribed in the algorithm. On the one hand, we used lower and higher thresholds for wind speed ( $\geq 10.8 \frac{\text{m}}{\text{s}}$  and  $\geq 17.2 \frac{\text{m}}{\text{s}}$ ) and “air-sea temperature difference” ( $\geq 39 \text{ K}$  and  $\geq 45 \text{ K}$ ) and on the other hand we left out the “air-sea temperature difference” and the “north south direction of the track” criterion, respectively. There is

a strong effect on the yearly numbers of detected polar lows (up to three times more cases when leaving the “north south direction of the track” criterion out), but no changes in the statistics: negligible trends and strong variability persist and the courses of the time series remain similar. Correlation coefficients are above  $\rho > 0.9$  between the times series

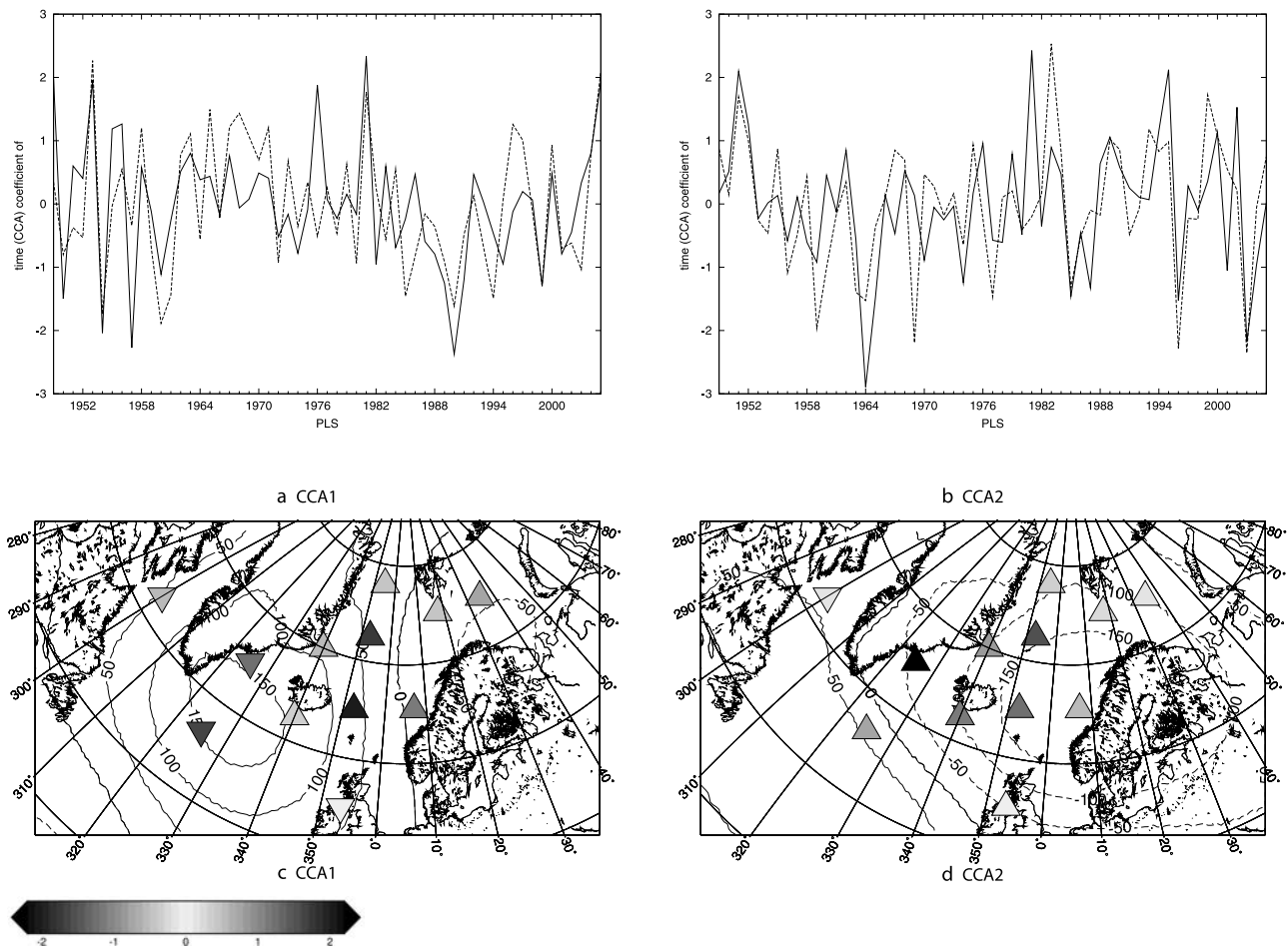


**Figure 3.** (a and b) First 2 Canonical coefficient time series and (c and d) corresponding correlation patterns between regional time series of polar low occurrences per PLS in regions R1–R12 (bold lines; triangles,  $\Delta$  for positive values,  $\nabla$  for negative values) and mean sea level pressure fields in Pa (dashed lines; isolines). The first CCA pair (Figures 3a and 3c) shares a correlation coefficient of 0.61 and represents 19% of the variance of the yearly number of occurrences. The second CCA pair (Figures 3b and 3d) shares a correlation of 0.58 and a variance of 24%.

gained with the varied thresholds and  $\rho \approx 0.8$  with the others.

### 3.2. Links to Large Scale Pressure Patterns

[18] Here we investigate how PLS-mean MSLP patterns are related to the distribution of yearly numbers of polar low occurrences. The PLS-mean MSLP fields are calculated consistently to the PLSs, namely as the mean field from July through June the following year. We consider this quantity because it is a large-scale, reliably and homogeneously analyzed field.

[19] Note that we do not compare the synoptic situation, as given by an instantaneous air pressure field, directly with the probability of a polar low to occur. Instead we indirectly relate the statistic of the “PLS mean MSLP field” with the statistic of the “number of Polar Lows” formed in different regions. Hence the mean state favors synoptic situations which condition polar low formation as a random realization of the short-term variability [cf. *Branstator, 1995; von Storch and Reichardt, 1997*].

[20] We quantify the linkage between the yearly mean MSLP-fields and the various regions’ polar low time series by means of Canonical Correlation Analysis (CCA) [von

*Storch and Zwiers, 1999*]. CCA is a method to calculate correlation between several multidimensional sets of variables. To exclude noise in each set we used the first 5 Empirical Orthogonal Functions (EOFs) of both the polar low time series on the one hand and the PLS-mean MSLP (representing 77% and 85% of the variance, respectively). We excluded the time series of R13 and R14, because there were too few polar lows occurring in these regions.

[21] Figure 3 shows the two most important combinations of patterns in terms of MSLP and polar low occurrence anomalies. Their coefficient time series (Figures 3a and 3b) share a correlation of about 0.60 - and thus may be degenerate, so that any linear combination of the two patterns would qualify. They both together describe about 40% of the year-to-year variance of polar low occurrences.

[22] The first Canonical pattern (CCA1, Figure 3c) describes a bipolar pressure distribution - when the CCA coefficient is positive then on average there will be a southward flow across the Norwegian Sea, and consistently, more polar lows. A pressure contrast of about 2 hPa between Northern Scandinavia and the region south of Greenland is associated with 0.5 to 1.6 less polar lows in the regions around south of Greenland (R5, R10, R12). In the



remaining regions of the North Atlantic, above normal polar low activity is found. Highest values of 1.7 and 2.0 appear in the regions in the pattern's central southward flow, R7 and R8. This pattern is reminiscent of the flow patterns found to be characteristic for marine cold air outbreaks in the these regions [Kolstad *et al.*, 2008]. Skeie [2000] suggests to call this anomalous circulation pattern "Barents Oscillation", as its center is located over the Barents Sea. When the sign of the coefficient changes, the pattern of additional and less polar lows reverses as well.

[23] A similar co-variability is described by the second pattern (Figure 3d), with a unipolar pattern centered over the Norwegian Sea and negative values below 1.5 hPa. Now the mean southward flow is shifted farther west compared to the first pattern. Accordingly highest values of 3.2 more polar lows show up in the region between Greenland and Iceland, R5.

[24] When examining the time series in Figures 3a and 3b, it is evident that CCA1 dominates the PLSs 1953, 1981 and 2005. In these PLSs noticeably high numbers of polar lows occur contemporaneously in the regions basically contributing to CCA1, R7, R8 and R9. Accordingly, minima of the time series correspond to years (e.g., 1954, 1990) with few polar low in all these regions.

[25] The second Canonical pattern (CCA2) is dominated by the region between Iceland and Greenland, R5. Thus CCA2 dominates in 1951 and 1995 with high numbers of polar lows in R5 and with a negative sign in 1964, 1996 and 2003 with markedly less polar lows in this region.

[26] We conducted the same investigations applying the mean MSLP field for the periods in which most of the polar lows occur, October through March. The results qualitatively stay the same, but numbers change to higher values. Now the former CCA2 pattern shares a correlation 0.74 and CCA1 shares a correlation of 0.64. The explained variances remain similar. The such gained time coefficients are similar those obtained based on the whole PLS ( $\rho > 0.85$ ).

[27] We conclude that a dynamical link exists between the occurrence of polar lows and time mean flow on time scales of years and longer, a significant link is associated only with anomalous meridional flow. The same analysis, with geopotential height at 500 hPa instead of MSLP, gave essentially the same results.

#### 4. Summary and Outlook

[28] For the first time a multidecadal LAM simulation was done with the purpose of deriving a climatology of polar lows in the subpolar North Atlantic.

[29] The 1949–2005 climatology shows large inter annual variability, but little decadal variability of polar low occurrences and no significant long-term changes in overall or regional polar low activity.

[30] By means of Canonical Correlation Analysis we determined MSLP patterns, averaged across a polar low year, which favor or disfavor the formation of spatial polar low occurrence. Meridional southward/poleward mean flows were found to establish large-scale time mean environments within which less/more polar lows develop.

[31] An important caveat with this study is that the model did not reproduce all polar lows of the real world; instead relevant statistics of polar low dynamics are realistically

reproduced - in particular the number of polar lows, their spatial distribution and the link to the time mean circulation are simulated consistently with the limited (typically: few years) observational evidence. The simulation is thus useful to analyze climatological issues of polar lows, but only to a limited extent for studying synoptic details of specific events.

[32] In this study we have used the data set only to assess year-to-year variability and possible trends. Beyond these issues, the space-time complete, digital data set has a high potential for the analysis of other issues, such as development mechanisms or the statistical linkage between polar low frequency and synoptic situations.

[33] **Acknowledgments.** Thanks to Eduardo Zorita for support with the statistical routines and to Dennis Bray for reading the manuscript. The work was conducted within the Virtual Institute (VI) EXTROP which is promoted by the "Initiative and Networking Fund" of the Helmholtz Association. NCEP Reanalysis data were provided by the NOAA/OAR/ESRL PSD, Boulder, Colorado, USA, from their Web site at <http://www.cdc.noaa.gov/>.

#### References

- Blechschmidt, A.-M. (2008), A 2-year climatology of polar low events over the Nordic seas from satellite remote sensing, *Geophys. Res. Lett.*, **35**, L09815, doi:10.1029/2008GL033706.
- Böhm, U., M. Kücken, W. Ahrens, A. Block, D. Hauffe, K. Keuler, B. Rockel, and A. Will (2006), CLM—The climate version of LM: Brief description and long-term applications, *COSMO NewsL.*, **6**, 225–235.
- Bracegirdle, T. J., and S. L. Gray (2008), An objective climatology of the dynamical forcing of polar lows in the Nordic seas, *Int. J. Climatol.*, **28**, 1903–1919, doi:10.1002/joc.1686.
- Branstator, G. (1995), Organization of storm track anomalies by recurring low-frequency circulation anomalies, *J. Atmos. Sci.*, **52**, 207–226.
- Businger, S. (1985), The synoptic climatology of polar low outbreaks, *Tellus, Ser. A*, **37**, 419–432.
- Claud, C., B. Duchiron, and P. Terray (2007), Associations between large-scale atmospheric circulation and polar low developments over the North Atlantic during winter, *J. Geophys. Res.*, **112**, D12101, doi:10.1029/2006JD008251.
- Condrón, A., G. R. Bigg, and I. A. Renfrew (2006), Polar mesoscale cyclones in the northeast Atlantic: Comparing climatologies from ERA-40 and satellite imagery, *Mon. Weather Rev.*, **134**(5), 1518–1533, doi:10.1175/MWR3136.1.
- Feser, F., and H. von Storch (2005), A spatial two-dimensional discrete filter for limited area model evaluation purposes, *Mon. Weather Rev.*, **133**(6), 1774–1786.
- Harold, J. M., G. R. Bigg, and J. Turner (1999), Mesocyclone activities over the north-east Atlantic. Part 1: Vortex distribution and variability, *Int. J. Climatol.*, **19**, 1187–1204.
- Kalnay, E., *et al.* (1996), The NCEP/NCAR 40-year reanalysis project, *Bull. Am. Meteorol. Soc.*, **77**(3), 437–471.
- Kolstad, E. (2006), A new climatology of favourable conditions for reverse-shear polar lows, *Tellus, Ser. A*, **58**, 344–354, doi:10.1111/j.1600-0870.2006.00171.x.
- Kolstad, E., T. J. Bracegirdle, and I. A. Seierstad (2008), Marine cold-air outbreaks in the North Atlantic: Temporal distribution and associations with large-scale atmospheric circulation, *Clim. Dyn.*, doi:10.1007/s00382-008-0431-5.
- Lystad, M. (Ed.) (1986), Polar lows in the Norwegian, Greenland and Barents Sea, final report, 196 pp., Norw. Meteorol. Inst., Oslo.
- Noer, G., and M. Ovsted (2003), Forecasting of polar lows in the Norwegian and the Barents Sea, paper presented at the 9th Meeting of the EGS Polar Lows Working Group, Eur. Geophys. Soc., Cambridge, U. K.
- Rasmussen, E., and J. Turner (2003), *Polar Lows: Mesoscale Weather Systems in the Polar Regions*, Cambridge Univ. Press, Cambridge, U. K.
- Simmons, A., and J. Gibson (2000), *The ERA-40 Project Plan, ERA-40 Proj. Rep. Ser.*, vol. 1, Eur. Cent. for Medium Range Weather Forecast., Reading, U. K.
- Skeie, P. (2000), Meridional flow variability over the Nordic seas in the Arctic Oscillation framework, *Geophys. Res. Lett.*, **27**, 2569–2572.
- von Storch, H., and H. Reichardt (1997), A scenario of storm surge statistics for the German Bight at the expected time of doubled atmospheric carbon dioxide concentration, *J. Clim.*, **10**, 2653–2662.
- von Storch, H., and F. Zwiers (1999), *Statistical Analysis in Climate Research*, 494 pp., Cambridge Univ. Press, New York.

- von Storch, H., H. Langenberg, and F. Feser (2000), A spectral nudging technique for dynamical downscaling purposes, *Mon. Weather Rev.*, *128*(10), 3664–3673.
- Wilhelmsen, K. (1985), Climatological study of gale-producing polar lows near Norway, *Tellus, Ser. A*, *37*, 451–459.
- Zahn, M., and H. von Storch (2008), Tracking polar lows in CLM, *Meteorol. Z.*, *17*(4), 445–453, doi:10.1127/0941-2948/2008/0317.
- Zahn, M., H. von Storch, and S. Bakan (2008), Climate mode simulation of North Atlantic polar lows in a limited area model, *Tellus, Ser. A*, *60*, 620–631, doi:10.1111/j.1600-0870.2008.00330.x.
- 
- H. von Storch and M. Zahn, Institute for Coastal Research, GKSS Research Center, Max-Planck-Straße 1, D-21502 Geesthacht, Germany. (matthias.zahn@gkss.de)